

## TURBULENT THERMAL DIFFUSION OF AEROSOLS IN GEOPHYSICS AND IN LABORATORY EXPERIMENTS

Alexander Eidelman, Tov Elperin, Nathan Kleorin, Alexander Krein, and Igor Rogachevskii  
*The Pearlstone Center for Aeronautical Engineering Studies, Department of Mechanical Engineering,  
The Ben-Gurion University of the Negev, POB 653, Beer-Sheva 84105, Israel*

Julia Buchholz and Gerd Grünefeld  
*Faculty of Mechanical Engineering, RWTH Aachen University, Aachen, Germany*  
(Dated: September 11, 2018)

We discuss a new phenomenon of turbulent thermal diffusion associated with turbulent transport of aerosols in the atmosphere and in laboratory experiments. The essence of this phenomenon is the appearance of a nondiffusive mean flux of particles in the direction of the mean heat flux, which results in the formation of large-scale inhomogeneities in the spatial distribution of aerosols that accumulate in regions of minimum mean temperature of the surrounding fluid. This effect of turbulent thermal diffusion was detected experimentally. In experiments turbulence was generated by two oscillating grids in two directions of the imposed vertical mean temperature gradient. We used Particle Image Velocimetry to determine the turbulent velocity field, and an Image Processing Technique based on an analysis of the intensity of Mie scattering to determine the spatial distribution of aerosols. Analysis of the intensity of laser light Mie scattering by aerosols showed that aerosols accumulate in the vicinity of the minimum mean temperature due to the effect of turbulent thermal diffusion.

### I. INTRODUCTION

Aerosols are a universal feature of the Earth's atmosphere. They can significantly affect the heat balance and dynamics of the atmosphere, climate, atmospheric chemistry, radiative transport and precipitation formation (see, e.g., Twomey, 1977; Seinfeld, 1986; Flagan and Seinfeld, 1988; Pruppacher and Klett 1997; Lohmann and Lesins, 2002; Kaufman et al. 2002; Anderson et al. 2003; and references therein). Formation of aerosol clouds is of fundamental significance in many areas of environmental sciences, physics of the atmosphere and meteorology (see, e.g., Seinfeld, 1986; Flagan and Seinfeld, 1988; Paluch and Baumgardner, 1989; Shaw et al. 1998; Shaw 2003; and references therein). It is well known that turbulence causes decay of inhomogeneities in spatial distribution of aerosols due to turbulent diffusion (see, e.g., Csanady, 1980; McComb 1990; Stock 1996), whereas the opposite effect, the preferential concentration of aerosols in atmospheric turbulence is not well understood.

Elperin et al. (1996; 1997; 1998; 2000b; 2001) recently found that in a turbulent fluid flow with a nonzero mean temperature gradient an additional mean flux of aerosols appears in the direction opposite to that of the mean temperature gradient, which is known as the phenomenon of turbulent thermal diffusion. This effect results in the formation of large-scale inhomogeneities in the spatial distribution of the aerosol particles.

The phenomenon of turbulent thermal diffusion is important for understanding atmospheric phenomena (e.g., atmospheric aerosols, smog formation, etc.). There exists a correlation between the appearance of tempera-

ture inversions and the aerosol layers (pollutants) in the vicinity of the temperature inversions (see, e.g., Seinfeld, 1986; Flagan and Seinfeld, 1988). Moreover, turbulent thermal diffusion can cause the formation of large-scale aerosol layers in the vicinity of temperature inversions in atmospheric turbulence (Elperin et al. 2000a; 2000c).

The main goal of this paper is to describe the experimental detection of a new phenomenon of turbulent thermal diffusion. To accomplish this, we constructed an oscillating grids turbulence generator (for details see Eidelman et al. 2002). Recent studies by De Silva and Fernando (1994); Srdic et al. (1996), Shy et al. (1997) have demonstrated the feasibility of generating nearly isotropic turbulence by two oscillating grids. Turbulent diffusion in oscillating grids turbulence was investigated by Ott and Mann (2000). In order to study turbulent thermal diffusion we used Particle Image Velocimetry to characterize a turbulent velocity field, and an Image Processing Technique based on Mie scattering to determine the spatial distribution of the particles. Our experiments were performed in two directions of the vertical mean temperature gradient: an upward mean temperature gradient (formed by a cold bottom and a hot top wall of the chamber) and a downward mean temperature gradient. We found that in a flow with a downward mean temperature gradient, particles accumulate in the vicinity of the top wall of the chamber (whereby the mean fluid temperature is minimal), and in a flow with an upward mean temperature gradient particles accumulate in the vicinity of the bottom wall of the chamber due to the effect of turbulent thermal diffusion.

The paper is organized as follows. Section II discusses

the physics of turbulent thermal diffusion, and Section III describes the experimental set-up for a laboratory study of this effect. The experimental results are presented in Section IV, and a detailed analysis of experimental detection of turbulent thermal diffusion is performed in Section V. Finally, conclusions are drawn in Section VI.

## II. TURBULENT THERMAL DIFFUSION

Evolution of the number density  $n(t, \mathbf{r})$  of small particles in a turbulent flow is determined by

$$\frac{\partial n}{\partial t} + \nabla \cdot (n \mathbf{v}_p) = -\nabla \cdot \mathbf{J}_M, \quad (1)$$

where  $\mathbf{J}_M$  is the molecular flux of the particles and  $\mathbf{v}_p$  is the velocity of the particles in the turbulent fluid velocity field. Averaging Eq. (1) over the statistics of the turbulent velocity field yields the following equation for the mean number density of particles  $\bar{N} \equiv \langle n \rangle$ :

$$\frac{\partial \bar{N}}{\partial t} + \nabla \cdot (\bar{N} \bar{\mathbf{V}}_p) = -\nabla \cdot (\bar{\mathbf{J}}_T + \bar{\mathbf{J}}_M), \quad (2)$$

$$\bar{\mathbf{J}}_T = \bar{N} \mathbf{V}_{\text{eff}} - D_T \nabla \bar{N}, \quad (3)$$

where  $D_T = (\tau/3)\langle \mathbf{u}^2 \rangle$  is the turbulent diffusion coefficient,  $\tau$  is the momentum relaxation time of the turbulent velocity field,  $\mathbf{v}_p = \bar{\mathbf{V}}_p + \mathbf{u}$ ,  $\bar{\mathbf{V}}_p = \langle \mathbf{v}_p \rangle$  is the mean particle velocity, and the effective velocity is

$$\mathbf{V}_{\text{eff}} = -\langle \tau \mathbf{u} (\nabla \cdot \mathbf{u}) \rangle. \quad (4)$$

Here  $\bar{\mathbf{J}}_M = -D(\nabla \bar{N} + k_t \nabla \bar{T}/\bar{T})$  is the mean molecular flux of particles,  $D$  is the coefficient of molecular diffusion,  $k_t$  is the thermal diffusion ratio, and  $\bar{T} = \langle T \rangle$  is the mean fluid temperature. Equations (2) and (3) were previously derived by different methods (see Elperin et al. 1996; 1997; 1998; 2000b; 2001; Pandya and Mashayek 2002).

For noninertial particles advected by a turbulent fluid flow, particle velocity  $\mathbf{v}_p$  coincides with fluid velocity  $\mathbf{v}$ , and  $\nabla \cdot \mathbf{v} \approx -(\mathbf{v} \cdot \nabla)\rho/\rho \approx (\mathbf{v} \cdot \nabla)T/T$ , where  $\rho$  and  $T$  are the density and temperature of the fluid. Thus, the effective velocity (4) for noninertial particles can be given by  $\mathbf{V}_{\text{eff}} = -D_T(\nabla \bar{T})/\bar{T}$ , which takes into account the equation of state for an ideal gas but neglects small gradients of the mean fluid pressure.

For inertial particles, velocity  $\mathbf{v}_p$  depends on the velocity of the surrounding fluid  $\mathbf{v}$ . Velocity  $\mathbf{v}_p$  can be determined by the equation of motion for a particle. Solving the equation of motion for a small solid particle with  $\rho_p \gg \rho$  yields:  $\mathbf{v}_p = \mathbf{v} - \tau_p d\mathbf{v}/dt + O(\tau_p^2)$  (see Maxey 1987), where  $\tau_p$  is the Stokes time and  $\rho_p$  is the material density of the particles. In that case

$$\nabla \cdot \mathbf{v}_p = \nabla \cdot \mathbf{v} + \tau_p \frac{\Delta P}{\rho} + O(\tau_p^2), \quad (5)$$

and the effective velocity of the inertial particles can be given by  $\mathbf{V}_{\text{eff}} = -D_T(1 + \kappa)(\nabla \bar{T})/\bar{T}$ , where  $P$  is the

fluid pressure. Coefficient  $\kappa$  depends on particle inertia ( $m_p/m_\mu$ ), the parameters of turbulence (Reynolds number) and the mean fluid temperature (Elperin et al. 1996; 1997; 1998; 2000b; 2001). Here  $m_p$  is the particle mass and  $m_\mu$  is the mass of molecules of the surrounding fluid. The turbulent flux of particles (3) can be rewritten as

$$\bar{\mathbf{J}}_T = -D_T \left[ k_T \frac{(\nabla \bar{T})}{\bar{T}} + \nabla \bar{N} \right], \quad (6)$$

where  $k_T = (1 + \kappa)\bar{N}$ . The first term in the RHS of Eq. (6) describes turbulent thermal diffusion, while the second term in the turbulent flux of particles (6) describes turbulent diffusion. Parameter  $k_T$  can be interpreted as the turbulent thermal diffusion ratio, and  $D_T k_T$  is the coefficient of turbulent thermal diffusion. Turbulent thermal diffusion causes the formation of a large-scale pattern wherein the initial spatial distribution of particles in a turbulent fluid flow evolves into a large-scale inhomogeneous distribution, i.e., particles accumulate in the vicinity of the minimum mean temperature of the surrounding fluid (Elperin et al. 1996; 1997; 1998; 2000b; 2001).

The mechanism responsible for the occurrence of turbulent thermal diffusion for particles with  $\rho_p \gg \rho$  can be described as follows. Inertia causes particles inside the turbulent eddies to drift out to the boundary regions between the eddies (i.e., regions with low vorticity or high strain rate and maximum of fluid pressure). Thus, particles accumulate in regions with maximum pressure of the turbulent fluid. For simplicity, let us consider a pure inertial effect, i.e., we assume that  $\nabla \cdot \mathbf{v} = 0$ . This inertial effect results in  $\nabla \cdot \mathbf{v}_p \propto \tau_p \Delta P \neq 0$ . On the other hand, Eq. (1) for large Peclet numbers yields  $\nabla \cdot \mathbf{v}_p \propto -dn/dt$ . The latter formula implies that  $dn/dt \propto -\tau_p \Delta P$ , i.e., inertial particles accumulate ( $dn/dt > 0$ ) in regions with maximum pressure of the turbulent fluid (where  $\Delta P < 0$ ). Similarly, there is an outflow of particles from regions with minimum pressure of fluid. In homogeneous and isotropic turbulence without large-scale external gradients of temperature, a drift from regions with increased or decreased concentration of particles by a turbulent flow of fluid is equiprobable in all directions, and pressure and temperature of the surrounding fluid do not correlate with the turbulent velocity field. Thus only turbulent diffusion of particles takes place.

In a turbulent fluid flow with a mean temperature gradient, the mean heat flux  $\langle \mathbf{u}\Theta \rangle$  is not zero, i.e., the fluctuations of fluid temperature  $\Theta = T - \bar{T}$  and the velocity of the fluid correlate. Fluctuations of temperature cause fluctuations of fluid pressure. These fluctuations result in fluctuations of the number density of particles. Indeed, an increase in pressure of the surrounding fluid is accompanied by an accumulation of particles. Therefore, the direction of the mean flux of particles coincides with that of the heat flux,  $\langle \mathbf{v}_p n \rangle \propto \langle \mathbf{u}\Theta \rangle \propto -\nabla \bar{T}$ , i.e., the mean flux of particles is directed to the area with minimum mean temperature, and the particles accumulate in that region.

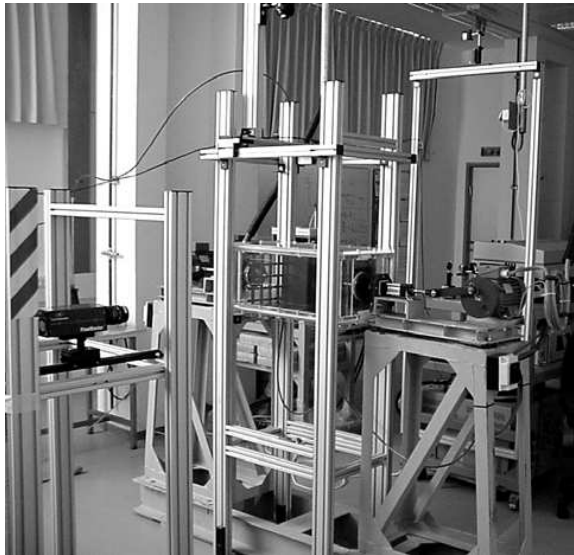


FIG. 1: The experimental set-up.



FIG. 2: The test section of the oscillating grids turbulence generator.

### III. EXPERIMENTAL SET-UP

In this Section we investigate experimentally the effect of turbulent thermal diffusion. The experiments were conducted in an oscillating grids turbulence generator in air flow (see Fig. 1). The test section consisted of a rectangular chamber of dimensions  $29 \times 29 \times 58$  cm (see Fig. 2). Pairs of vertically oriented grids with bars arranged in a square array were attached to the right and left horizontal rods. Both grids were driven independently with speed-controlled motors. The grids were positioned at a distance of two-grid meshes from the chamber walls parallel to them. A two-grid system can oscillate at a controllable frequency up to 20 Hz. The grid stroke was adjusted within a range of 1 to 10 cm.

A vertical mean temperature gradient in the turbulent

flow was formed by attaching two aluminium heat exchangers to the bottom and top walls of the test section (see Fig. 2). The experiments were performed in two directions of the mean temperature gradient: an upward mean temperature gradient (a cold bottom and a hot top wall of the chamber) and a downward mean temperature gradient (a heated bottom and a cold top wall of the chamber). In order to improve the heat transfer in the boundary layers at the walls we used a heat exchanger with rectangular pins  $3 \times 3 \times 15$  mm. This allowed us to support a mean temperature gradient in the core of the flow up to 200 K/m in the upward direction and up to 110 K/m in the downward direction at a mean temperature of about 300 K. The temperature was measured with a high-frequency response thermocouple.

The velocity field was measured using a Particle Image Velocimetry (PIV), see Raffel et al. (1998). A digital PIV system with LaVision Flow Master III was used. A double-pulsed light sheet was provided by a Nd-YAG laser source (Continuum Surelite  $2 \times 170$  mJ). The light sheet optics includes spherical and cylindrical Galilei telescopes with tuneable divergence and adjustable focus length. We used a progressive-scan 12 bit digital CCD camera (pixel size  $6.7 \mu\text{m} \times 6.7 \mu\text{m}$  each) with a dual-frame-technique for cross-correlation processing of captured images. A programmable Timing Unit (PC interface card) generated sequences of pulses to control the laser, camera and data acquisition rate. The software package DaVis 6 was applied to control all hardware components and for 32 bit image acquisition and visualization. This software package contains PIV software for calculating the flow fields using cross-correlation analysis. Velocity maps and their characteristics, e.g., statistics and PDF, were analyzed with this package plus an additional developed software package. An incense smoke with sub-micron particles (with  $\rho_p/\rho \sim 10^3$ ) as a tracer was used for the PIV measurements. Smoke was produced by high temperature sublimation of solid incense particles. Analysis of smoke particles using a microscope (Nikon, Epiphot with an amplification of 560) and a PM-300 portable laser particulate analyzer showed that these particles have a spherical shape and that their mean diameter is  $0.7 \mu\text{m}$ .

Mean and r.m.s. velocities, two-point correlation functions and an integral scale of turbulence from the measured velocity fields were determined. A series of 100 pairs of images acquired with a frequency of 4 Hz were stored for calculating the velocity maps and for ensemble and spatial averaging of turbulence characteristics. The center of the measurement region coincides with the center of the chamber. We measured the velocity for flow areas from  $60 \times 60 \text{ mm}^2$  up to  $212 \times 212 \text{ mm}^2$  with a spatial resolution of  $1024 \times 1024$  pixels. This size of the probed area corresponds to a spatial resolution from  $58 \mu\text{m} / \text{pixel}$  up to  $207 \mu\text{m} / \text{pixel}$ . These regions were analyzed with interrogation windows of  $32 \times 32$  and  $16 \times 16$  pixels. A velocity vector was determined in every interrogation window, allowing us to construct a velocity

map comprising  $32 \times 32$  or  $64 \times 64$  vectors. The velocity maps were determined in two planes. In the one-grid experiments the plane was parallel to the grid, while in the two-grid experiments the plane was normal to the grids. The mean and r.m.s. velocities for each point of the velocity map (1024 points) were determined by averaging over 100 independent maps, and then over 1024 points. The two-point correlation functions of the velocity field were determined for each point of the central part of the velocity map ( $16 \times 16$  vectors) by averaging over 100 independent velocity maps, and then over 256 points. An integral scale  $L$  of turbulence was determined from the two-point correlation functions of the velocity field. These measurements were repeated for different distances from the grid, and for various temperature gradients, Reynolds numbers and particle mass loadings. The PIV measurements performed in the oscillating grids turbulence generator confirmed earlier results (Thompson and Turner 1975; Hopfinger and Toly 1976; Kit et al. 1997) for the dependence of various characteristics of the turbulent velocity field on the parameters of the oscillating grids turbulence generator.

To determine the spatial distribution of the particles, we used an Image Processing Technique based on Mie scattering. The advantages of this method have been demonstrated by Guibert et al. (2001). The light radiation energy flux scattered by small particles is  $E_s \propto \tilde{E} \Psi(\pi d_p/\lambda; a; n)$ , where  $\tilde{E} \propto \pi d_p^2/4$  is the energy flux incident at the particle,  $d_p$  is the particle diameter,  $\lambda$  is the wavelength,  $a$  is the index of refraction and  $\Psi$  is the scattering function. In the general case,  $\Psi$  is given by Mie equations. For wavelengths  $\lambda$ , which are smaller than the particle size,  $\Psi$  tends to be independent of  $d_p$  and  $\lambda$ . The scattered light energy flux incident on the CCD camera probe is proportional to the particle number density  $n$ , i.e.,  $E_s \propto \tilde{E} n(\pi d_p^2/4)$ .

Mie scattering does not change from temperature effects since it depends on the permittivity of particles, the particle size and the laser light wavelength. The effect of the temperature on these characteristics is negligibly small. Note that in each experiment before taking the measurements, we let the system run for some time (up to 30 minutes after smoke injection into the flow with a steady mean temperature profile) in order to attain a stationary state.

We found that the probability density function of the particle size measured with the PM300 particulate analyzer was to the most extent independent of the location in the flow for incense particle size of  $0.5 - 1 \mu\text{m}$ . Note that since the number density of the particles is small (about 1 mm apart), it can be assumed that a change in particle number density will not affect their size distribution. Therefore, the ratio of the scattered radiation fluxes at two points and at the image measured with the CCD camera remains equal to the ratio of the particle mean number densities at these two locations.

#### IV. EXPERIMENTAL DETECTION OF TURBULENT THERMAL DIFFUSION

The turbulent flow parameters in the oscillating grids turbulence generator are: r.m.s. velocity  $\sqrt{\langle \mathbf{u}^2 \rangle} = 4 - 14$  cm/s depending on the frequency of the grid oscillations, integral scale of turbulence  $L = 1.6 - 2.3$  cm, and the Kolmogorov length scale  $\eta = 380 - 600 \mu\text{m}$ . Other parameters are given in Section 5 (Tables 1-2). These flows involve a wide range of scales of turbulent motions. Interestingly, a flow with a wide range of spatial scales is already formed at comparatively low frequencies of grid oscillations. We found a weak mean flow in the form of two large toroidal structures parallel and adjacent to the grids. The interaction of these structures results in a symmetric mean flow that is sensitive to the parameters of the grid adjustments. We particularly studied the parameters that affect a mean flow such as the grid distance to the walls of the chamber and partitions, and the angles between the grid planes and the axes of their oscillations. Varying these parameters allowed us to expand the central region with a homogeneous turbulence. We found that the measured r.m.s. velocity was several times higher than the mean velocity in the core of the flow.

The temperature measurements were taken in the oscillating grids turbulence generator. The temperature difference between the heat exchangers varied within a range of 25 to 50 K. The mean temperature vertical profiles at a frequency of grids oscillations  $f = 10.5$  Hz in turbulent flows with downward and upward mean temperature gradients are shown in Fig. 3. Here  $Z$  is a dimensionless vertical coordinate measured in units of the height of the chamber, and  $Z = 0$  at the bottom of the chamber. Hereafter, we use the following system of coordinates:  $Z$  is the vertical axis, the  $Y$ -axis is perpendicular to the grids and the  $XZ$ -plane is parallel to the grids plane.

Measurements performed using different concentrations of incense smoke showed that in an isothermal flow the distribution of the average scattered light intensity over a vertical coordinate is independent of the mean particle number density. In order to characterize the spatial distribution of particle number density  $\bar{N} \propto E^T/E$  in a non-isothermal flow, the distribution of the scattered light intensity  $E$  for the isothermal case was used to normalize the scattered light intensity  $E^T$  obtained in a non-isothermal flow under the same conditions. The scattered light intensities  $E^T$  and  $E$  in each experiment were normalized by corresponding scattered light intensities averaged over the vertical coordinate. The ratios  $E^T/E$  of the normalized average distributions of the intensity of scattered light as a function of the normalized vertical coordinate  $Z$  in turbulent flows with a downward mean temperature gradient and with an upward mean temperature gradient are shown in Fig. 4. The figure demonstrates that particles are redistributed in a turbulent flow with a mean temperature gradient. Particles accumulate

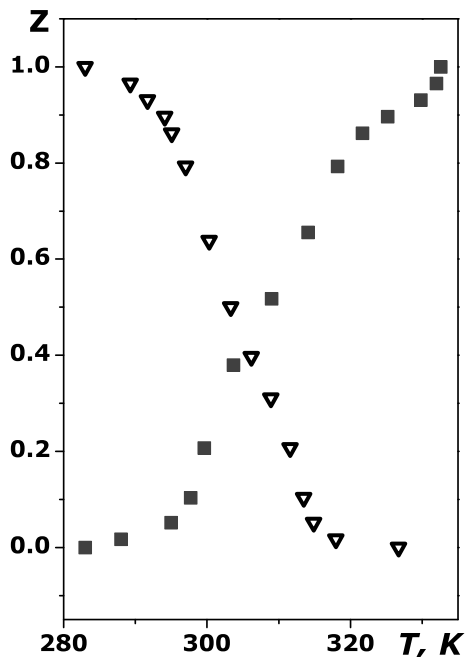


FIG. 3: Vertical temperature profiles at frequency of grid oscillations  $f = 10.5$  Hz in turbulent flows with an upward mean temperature gradient (filled squares) and with a downward mean temperature gradient (unfilled triangles). Here  $Z$  is a dimensionless vertical coordinate measured in units of the height of the chamber, and  $Z = 0$  at the bottom of the chamber.

in regions of minimum mean temperature (in the lower part of the chamber in turbulent flows with an upward mean temperature gradient), and there is an outflow of particles from the upper part of the chamber where the mean temperature is larger. On the other hand, in a flow with a downward mean temperature gradient (a hot bottom and a cold top wall of the test section) particles accumulate in the vicinity of the top wall of the chamber, i.e., in the vicinity where the mean fluid temperature is minimum.

To determine the turbulent thermal diffusion ratio, we plotted the normalized particle number density  $N_r \equiv \bar{N}/\bar{N}_0$  versus the normalized temperature difference  $T_r \equiv (\bar{T} - \bar{T}_0)/\bar{T}_0$ , where  $\bar{T}_0$  is the reference temperature and  $\bar{N}_0 = \bar{N}(\bar{T} = \bar{T}_0)$ . The function  $N_r(T_r)$  is shown in Fig. 5 for a turbulent flow with an upward mean temperature gradient and in Fig. 6 for a turbulent flow with a downward mean temperature gradient.

We probed the central  $20 \times 20$  cm region in the chamber by determining the mean intensity of scattered light in  $32 \times 16$  interrogation windows with a size of  $32 \times 64$  pixels. The vertical distribution of the intensity of the scat-

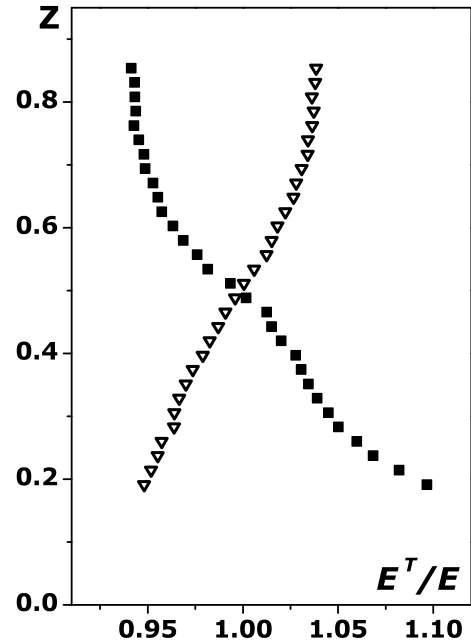


FIG. 4: Ratios  $E^T/E$  of normalized average distributions of the intensity of scattered light versus the normalized vertical coordinate  $Z$  in turbulent flows with an upward mean temperature gradient (filled squares) and with a downward mean temperature gradient (unfilled triangles). Here  $Z = 0$  is at the bottom of the chamber. The frequency of grids oscillations is  $f = 10.5$  Hz.

tered light was determined in 16 vertical strips, which are composed of 32 interrogation windows. Variations of the obtained vertical distributions between these strips were very small. Therefore in Figs. 4-6 we used spatial average over strips and the ensemble average over 100 images of the vertical distributions of the intensity of scattered light. Figures 5-6 were plotted using the mean temperature vertical profiles shown in Fig. 3. The normalized local mean temperatures [the relative temperature differences  $(\bar{T} - \bar{T}_0)/\bar{T}_0$ ] in Figs. 5-6 correspond to the different points inside the probed region. In particular, in Fig. 5 the location of the point with reference temperature  $\bar{T}_0$  is  $Z = 0.135$  (the lowest point of the probed region with a maximum  $\bar{N}$  in turbulent flows with an upward mean temperature gradient), and the point with a maximum normalized temperature difference is the highest point of the probed region at  $Z = 0.865$ . The size of the probed region did not affect our results.

## V. DISCUSSION

The vertical profiles of the mean number density of particles obtained in our experiments can be explained

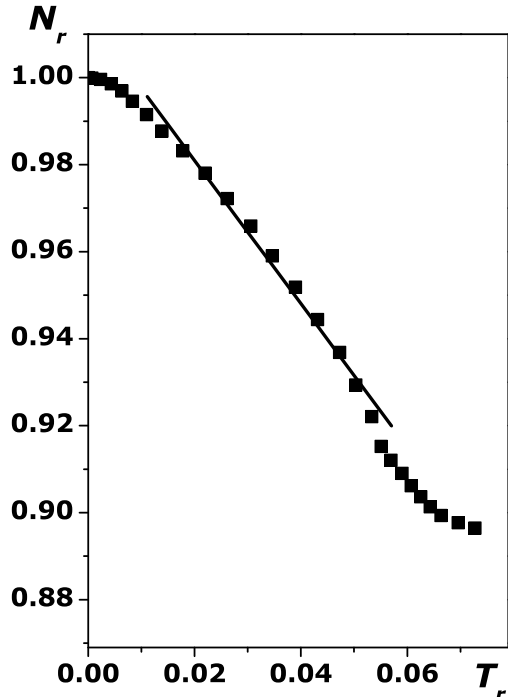


FIG. 5: Normalized particle number density  $N_r \equiv \bar{N}/\bar{N}_0$  versus normalized temperature difference  $T_r \equiv (\bar{T} - \bar{T}_0)/\bar{T}_0$  in a turbulent flow with an upward mean temperature gradient. The frequency of grid oscillations is  $f = 10.5$  Hz.

by considering Eqs. (2) and (3). If one does not take into account the term  $\bar{N}\mathbf{V}_{\text{eff}}$  in Eq. (2) for the mean number density of particles, the equation reads  $\partial\bar{N}/\partial t = D_r\Delta\bar{N}$ , where we neglected a small mean fluid velocity  $\bar{\mathbf{V}}_p$  and a small molecular mean flux of particles (that corresponds to the conditions of the experiment). The steady-state solution of this equation is  $\bar{N} = \text{const}$ . However, our measurements demonstrate that the solution  $\bar{N} = \text{const}$  is valid only for an isothermal turbulent flow, i.e., when  $\bar{T} = \text{const}$ . By taking into account the effect of turbulent thermal diffusion, i.e., the term  $\bar{N}\mathbf{V}_{\text{eff}}$  in Eq. (2), the steady-state solution of this equation for non-inertial particles is:  $\nabla\bar{N}/\bar{N} = -\nabla\bar{T}/\bar{T}$ . The latter equation yields  $\bar{N}/\bar{N}_0 = 1 - (\bar{T} - \bar{T}_0)/\bar{T}_0$ , where  $\bar{T} - \bar{T}_0 \ll \bar{T}_0$ . In the experiments using particles of the size  $0.5 - 2 \mu\text{m}$ , we found that

$$\frac{\bar{N}}{\bar{N}_0} = 1 - \alpha \frac{\bar{T} - \bar{T}_0}{\bar{T}_0}, \quad (7)$$

where the coefficient  $\alpha = 1.33 - 1.79$  (depending on the frequency of the grid oscillations) in a turbulent flow with an upward mean temperature gradient, and  $\alpha = 1.29 - 1.87$  in a turbulent flow with a downward mean temperature gradient (see Tables 1-2). The deviation of coefficient  $\alpha$  from 1 is caused by a small yet finite inertia

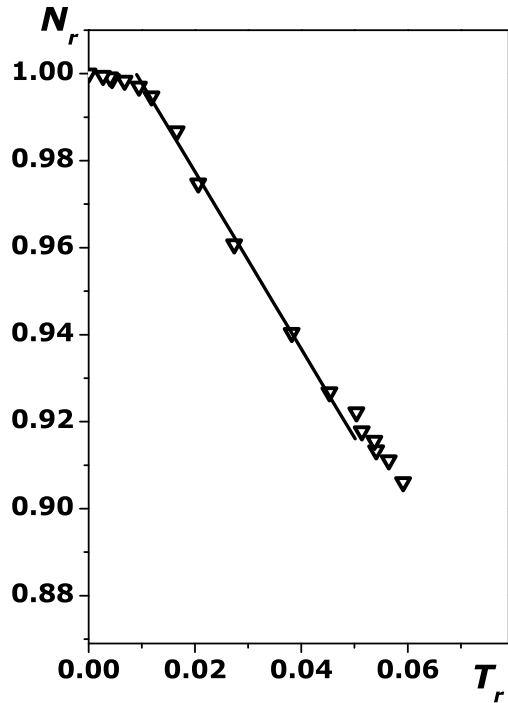


FIG. 6: Normalized particle number density  $N_r \equiv \bar{N}/\bar{N}_0$  versus normalized temperature difference  $T_r \equiv (\bar{T} - \bar{T}_0)/\bar{T}_0$  in a turbulent flow with a downward mean temperature gradient. The frequency of grid oscillations is  $f = 10.4$  Hz.

of the particles and by the dependence of coefficient  $\alpha$  on the mean temperature gradient. The exact value of parameter  $\alpha$  for inertial particles cannot be found within the framework of the theory of turbulent thermal diffusion (Elperin et al. 1996; 1997; 1998; 2000b; 2001) for the conditions of our experiments (i.e., for strong mean temperature gradients). However, in all the present experiments performed for different ranges of parameters and different directions of a mean temperature gradient, the coefficient of turbulent thermal diffusion  $\alpha$  was more than 1, which does agree with the theory. In particular, the theory predicts  $\alpha = 1$  for noninertial particles, and  $\alpha > 1$  for inertial particles. As can be seen in Tables 1-2, parameter  $\alpha$  slightly decreases when the Reynolds number increases.

There are other factors that can affect the spatial distribution of particles. The contribution of the mean flow to the spatial distribution of particles is negligibly small. Indeed, the normalized distribution of the scattered light intensity measured in the different vertical strips in the regions where the mean flow velocity and the coefficient of turbulent diffusion vary strongly are practically identical (the difference being only about 1%). Due to the effect of turbulent thermal diffusion, particles are redistributed in the vertical direction in the chamber. In turbulent

$f$ (Hz)	$\sqrt{\langle \mathbf{u}^2 \rangle}$ (cm/s)	$L$ (cm)	Re	$\alpha$
6.5	3.6	1.9	46	1.79
10.5	7.2	2.1	101	1.65
14.5	10.7	2.3	164	1.43
16.5	12.4	2.0	165	1.33

TABLE I: Parameters of turbulence and the turbulent thermal diffusion coefficient for a turbulent flow with an upward mean temperature gradient. Here  $\text{Re} = L \sqrt{\langle \mathbf{u}^2 \rangle} / \nu$ ,  $L$  is the integral scale of turbulence, and  $\nu$  is the kinematic viscosity.

$f$ (Hz)	$\sqrt{\langle \mathbf{u}^2 \rangle}$ (cm/s)	$L$ (cm)	Re	$\alpha$
8.4	8.8	1.85	109	1.87
10.4	9.7	1.75	113	1.60
12.4	11.1	1.65	122	1.69
14.4	11.7	1.84	144	1.34
16.4	14.0	1.64	153	1.29

TABLE II: Parameters of turbulence and the turbulent thermal diffusion coefficient for a turbulent flow with a downward mean temperature gradient.

flows with an upward mean temperature gradient particles accumulated in the lower part of the chamber, and in flows with a downward mean temperature gradient particles accumulated in the vicinity of the top wall of the chamber, i.e., in regions with a minimum mean temperature. The spatial-temporal evolution of the normalized number density of particles  $N_r$  is governed by the conservation law of the total number of particles (see Eqs. (2) and (3)). Some fraction of particles sticks to the walls of the chamber, and the total number of particles without feeding fresh smoke slowly decreases. The characteristic time of this decrease is about 15 minutes. However, the spatial distribution of the normalized number density of particles does not change over time.

The number density of particles in our experiments was of the order of  $10^{10}$  particles per cubic meter. Therefore, the distance between particles is about 1 mm, and their collision rate is negligibly small. Indeed, calculation of

the particle collision rate using the Saffman-Turner formula (Saffman and Turner 1956) confirmed this finding. Consequently, we did not observe any coalescence of particles. The effect of the gravitational settling of small particles ( $0.5 - 1 \mu\text{m}$ ) is negligibly small (the terminal fall velocity of these particles being less than  $0.01 \text{ cm/s}$ ). Thus, we may conclude that the two competitive mechanisms of particle transport, i.e., mixing by turbulent diffusion and accumulation of particles due to turbulent thermal diffusion, exist simultaneously and there is a very small effect of gravitational settling of the particles.

In regard to the accuracy of the performed measurements, we found that uncertainties in optics adjustment and errors in measuring a CCD image background value are considerably less than the observed effect of a 10% change of normalized intensity of the scattered light in the test section in the presence of an imposed mean temperature gradient. In the range of the tracer concentrations used in the experiments the particle-air suspension can be considered as an optically thin medium, from which we can infer that the intensity of the scattered light is proportional to the particle number density. The total error in our measurements was determined by  $(\delta\bar{N}/\bar{N} + \delta\bar{T}/\bar{T})/\sqrt{Q} \approx 0.3\%$  (see Eq. (7)), where  $\delta\bar{T} = 0.1K$  is the accuracy of the temperature measurements;  $\delta\bar{N}/\bar{N} = 0.8\%$  is the accuracy of the mean number density measurements; and  $Q = 8$  is the number of experiments performed for each direction of the mean temperature gradient and for each value of the frequency of the grid oscillations. The total variation of the normalized particle number density due to the effect of turbulent thermal diffusion is more than 10% (see Figs. 4-6). The relative error of the measurements is less than 3% of the total variation of the particle number density. Thus, the accuracy of these measurements is considerably higher than the magnitude of the observed effect. As such, our experiments confirm the existence of an effect of turbulent thermal diffusion, as predicted theoretically by Elperin et al. (1996; 1997).

## VI. CONCLUSIONS

A new phenomenon of turbulent thermal diffusion has been detected experimentally in turbulence generated by oscillating grids with an imposed vertical mean temperature gradient in air flow. This phenomenon implies that there exists an additional mean flux of particles in the direction opposite to that of the mean temperature gradient, that results in the formation of large-scale inhomogeneities in the spatial distribution of particles. The particles accumulated in the vicinity of the minimum mean fluid temperature. In the experiments in two directions of the vertical mean temperature gradient, it was found that in a flow with a downward mean temperature gradient particles accumulate in the vicinity of the top wall of the chamber. In a flow with an upward mean temperature gradient particles accumulate in the vicinity of the

bottom wall of the chamber. Turbulent thermal diffusion can explain the large-scale aerosol layers that form inside atmospheric temperature inversions.

### Acknowledgments

We are indebted to F. Busse, H. J. S. Fernando, J. Katz, E. Kit, V. L'vov, J. Mann, S. Ott and A. Tsi-

nober for illuminating discussions. We also thank A. Markovich for his assistance in processing the experimental data. This work was partially supported by the German-Israeli Project Cooperation (DIP) administered by the Federal Ministry for Education and Research (BMBF) and by the Israel Science Foundation governed by the Israeli Academy of Science.

- 
- [1] Anderson, L., Charlson, R. J., Schwartz, S. E., Knutti, R., Boucher, O., Rodhe, H. and Heintzenberg, J., Climate forcing by aerosols - a hazy picture, *Science*, *300*, 1103-1104, 2003.
- [2] Csanady, G. T., *Turbulent Diffusion in the Environment*, Reidel, Dordrecht, 1980.
- [3] De Silva, I. P. D. and Fernando H. J. S., Oscillating grids as a source of nearly isotropic turbulence, *Phys. Fluids*, *6*., 2455-2464, 1994.
- [4] Eidelman, A., Elperin, T., Kapusta, A., Kleeorin, N., Krein, A. and Rogachevskii, I., Oscillating grids turbulence generator for turbulent transport studies, *Nonlinear Processes in Geophysics*, *9*, 201-205, 2002.
- [5] Elperin, T., Kleeorin, N. and Rogachevskii, I., Turbulent thermal diffusion of small inertial particles, *Phys. Rev. Lett.*, *76*, 224-228, 1996.
- [6] Elperin, T., Kleeorin, N. and Rogachevskii, I., Turbulent barodiffusion, turbulent thermal diffusion and large-scale instability in gases, *Phys. Rev. E*, *55*, 2713-2721, 1997.
- [7] Elperin, T., Kleeorin, N. and Rogachevskii, I., Formation of inhomogeneities in two-phase low-mach-number compressible turbulent flows, *Int. J. Multiphase Flow*, *24*, 1163-1182, 1998.
- [8] Elperin, T., Kleeorin, N. and Rogachevskii, I., Mechanisms of formation of aerosol and gaseous inhomogeneities in the turbulent atmosphere, *Atmosph. Res.*, *53*, 117-129, 2000a.
- [9] Elperin, T., Kleeorin, N., Rogachevskii, I. and Sokoloff, D., Passive scalar transport in a random flow with a finite renewal time: mean-field equations, *Phys. Rev. E*, *61*, 2617-2625, 2000b.
- [10] Elperin, T., Kleeorin, N., Rogachevskii, I. and Sokoloff, D., Turbulent transport of atmospheric aerosols and formation of large-scale structures, *Physics and Chemistry of the Earth*, *A25*, 797-803, 2000c.
- [11] Elperin, T., Kleeorin, N., Rogachevskii, I. and Sokoloff, D., Mean-field theory for a passive scalar advected by a turbulent velocity field with a random renewal time, *Phys. Rev. E*, *64*, 026304 (1-9), 2001.
- [12] Flagan, R. and Seinfeld, J. H., *Fundamentals of Air Pollution Engineering*, Prentice Hall, Englewood Cliffs, 1988.
- [13] Guibert, P., Durget, M. and Murat, M., Concentration fields in a confined two-gas mixture and engine in cylinder flow: laser tomography measurements by Mie scattering., *Exp. Fluids*, *31*, 630-642, 2001.
- [14] Hopfinger, E. J. and Toly, J.-A., Spatially decaying turbulence and its relation to mixing across density interfaces, *J. Fluid Mech.*, *78*, 155-175, 1976.
- [15] Kaufman, Y. J., Tanre, D. and Boucher, O., A satellite view of aerosols in the climate system, *Nature*, *419*, 215-223, 2002.
- [16] Kit, E., Strang, E. J. and Fernando, H. J. S., Measurement of turbulence near shear-free density interfaces, *J. Fluid Mech.*, *334*, 293-314, 1997.
- [17] Lohmann, U. and Lesins, G., Stronger constraints on the anthropogenic indirect aerosol effect. *Science*, *298*, 1012-1015, 2002.
- [18] Maxey, M. R., The gravitational settling of aerosol particles in homogeneous turbulence and random flow field, *J. Fluid Mech.*, *174*, 441-465, 1987.
- [19] McComb, W. D., *The Physics of Fluid Turbulence*, Clarendon, Oxford, 1990.
- [20] Ott, S. and Mann, J., An experimental investigation of the relative diffusion of particle pairs in three-dimensional turbulent flow, *J. Fluid Mech.*, *422*, 207-234, 2000.
- [21] Pandya, R. V. R. and Mashayek, F., Turbulent thermal diffusion and barodiffusion of passive scalar and dispersed phase of particles in turbulent flows, *Phys. Rev. Lett.*, *88*, 044501 (1-4), 2002.
- [22] Paluch, I. R., and Baumgardner, D. G., Entrainment and fine-scale mixing in a continental convective cloud, *J. Atmos. Sci.*, *46*, 261-278, 1989.
- [23] Pruppacher, H. R. and Klett, J. D., *Microphysics of Clouds and Precipitation*, Kluwer Acad. Publ., Dordrecht, 1997.
- [24] Raffel, M., Willert, C. and Kompenhans, J., *Particle Image Velocimetry*. Springer, 1998.
- [25] Saffman, P. G. and Turner, J. S., On the collision of drops in turbulent clouds, *J. Fluid Mech.*, *1*, 16-30, 1956.
- [26] Seinfeld, J. H., *Atmospheric Chemistry and Physics of Air Pollution*, John Wiley, New York, 1986.
- [27] Shaw, R. A., Reade, W. C., Collins L. R. and Verlinder J., Preferential concentration of cloud droplets by turbulence: effects on the early evolution of cumulus cloud droplet spectra. *J. Atmosph. Sci.*, *55*, 1965-1976, 1998.
- [28] Shaw, R. A., Particle-turbulence interactions in atmospheric clouds, *Ann. Rev. Fluid Mech*, *35*, pp. 183-227, 2003.
- [29] Shy, S. S., Tang, C. Y. and Fann, S. Y., A nearly isotropic turbulence generated by a pair of vibrating grids, *Exp. Thermal Fluid Sci.*, *14*, 251-262, 1997.
- [30] Srdic, A., Fernando, H. J. S. and Montenegro, L., Generation of nearly isotropic turbulence using two oscillating grids. *Exper. in Fluids*, *20*, 395-397, 1996.
- [31] Stock, D., Particle dispersion in flowing gases, *ASME J. Fluids Engineering*, *118*, 4-17, 1996.
- [32] Telford, J. W., Clouds with turbulence: the role of entrainment. *Atmos. Res.*, *40*, 261-282, 1996.

- [33] Thompson, S. M. and Turner, J. S., Mixing across an interface due to turbulence generated by an oscillating grid, *J. Fluid Mech.*, *67*, 349-368, 1975.
- [34] Twomey, S., *Atmospheric Aerosols*, Elsevier, Amsterdam, 1977.